IOSR Journal of Applied Geology and Geophysics (IOSR-JAGG)
e-ISSN: 2321–0990, p-ISSN: 2321–0982.Volume 11, Issue 6 Ser. I (Nov. – Dec. 2023), 01-11
www.iosrjournals.org

Detection and Classification of Vertical Objects in Point Cloud Data for Urban Planning and Management

Elizabete Bugalski de Andrade Peixoto[1], Jorge Antonio da Silva Centeno[2]
[1,2](Departament of Geociences, PPGCG/UFPR)/ Federal University of Paraná, Brazil)

***Abstract*:**
Over the last years, several methods have been developed to collect point clouds that enable describing objects, which can support mapping and understanding urban furniture for urban planning and management. Considering the data volume, automatic methods are needed to speed up the object extraction from the point cloud. In this paper it is introduced a method for detecting and classifying poles using point cloud data acquired from a mobile terrestrial laser scanner. First, the 2D density is analyzed to locate and segment the probable objects. Then the geometry of the pole is modeled. The detected objects were further categorized into their respective top and pole components, and relevant variables were calculated for classification using a neural network. The results of this research demonstrate the effectiveness of utilizing point cloud data for the detection and identification of vertical objects. By leveraging the density analysis and segmentation techniques, accurate detection and classification of poles and road signs were achieved. This methodology has the potential to improve the efficiency and accuracy of feature detection in various applications that rely on point cloud data.
Keywords: *Point Cloud, Mobile Terrestrial Laser, Detection, Classification, Neural Networks, Poles and Signs*

Date of Submission: 29-10-2023 Date of Acceptance: 09-11-2023

I. Introduction

Investments in infrastructure have gained significant attention worldwide, driven by the need to enhance urban mobility and support rational development (Dias, 2018). As the urban environment is very dynamic, there is the need for a constant mapping of urban furniture, aiming at assessing the existence or need of several basic infrastructure, like poles or information shields. In the last decade, collecting point clouds became a common practice in the surveying field, using photogrammetry or LiDAR. The availability of dense point clouds demands the development of new methods to process them and extract valuable information, such as the segmentation and classification of poles and shields. For instance, through the utilization of a mobile terrestrial LiDAR system, an extensive dataset can be acquired, capturing detailed 3D information of the surroundings. This dataset serves as the foundation for developing an efficient detection and classification methodology. The application of LiDAR technology enables remote sensing, ensuring non-contact data acquisition and providing advantages in terms of safety and data accuracy.

While numerous classification methods exist, LiDAR point cloud classification is particularly complex due to the similarities between different objects (Fernandes et al., 2021). Consequently, it remains a subject of intensive research. In this context, the focus of this study is on the semi-automatic detection and classification of poles, and objects attached to them, like road signs, using Mobile Terrestrial LiDAR and a neural network-based approach.

The pioneering work of (Manandhar and Shibasaki, 2001) focused on mapping objects along roads using Mobile Terrestrial LiDAR (MTL). They used a system composed by six cameras, three LiDAR units, and a Hybrid Inertial Survey System (HISS), consisting of DGPS, INS and an odometer. One of the aims of their research was to extract objects from the 3D point cloud without any spectral information. The main objective was the extraction of facades of the buildings, trees and roads. The objects were classified into two classes: artificial and natural, based on the point cloud dispersion (scattering), as natural objects have more irregular geometric shape than artificial ones. To analyze the dispersion of the points in three dimensions, they computed the second derivative of the distance. The study proved that the variation of distance is greater in natural features, such as trees, and smaller in artificial features such as buildings, walls, and roads.

In another study, (Chen et al., 2007) employed a system consisting of three sensor, laser, CCD cameras and a fixed GPS/IMU/VMS navigation platform. The laser equipment used was the LMS 200, which is a two-dimensional laser, with maximum range of 80 meters and an average resolution of 30 mm. The navigation platform used is composed of a DGPS, an IMU and a VMS (Velocity measurement system). To extract vertical objects, like poles, their linear characteristic was considered. All objects were projected onto a 2D horizontal

plane, where clusters were identified, considering that each cluster is caused by the vertical projection of several points on their surface. Then, the principal components of each cluster were analyzed to detect poles or shields.

Carried out in urban environments, (Golovinski et al., 2009) conducted a project to recognize objects from 3D point cloud. The project was divided down into four steps: location, segmentation, characterization, and classification of 3D clusters. First, neighboring points are grouped together into clusters with a potential chance of being an object, a hierarchical grouping. Then the points were classified as belonging to the foreground and background, and a feature vector was computed for each group of foreground points. Finally, the vectors were labeled using a supervised classifier. They tested and compared several methods at each step. The application of multiple segmentation methods provides different results and therefore a greater variety of features can be used in the classification step. Segments were classified by applying the nearest neighbor, Randon Forest and SVM (Support Vector Machine) algorithms. Through the experiments, it was proven that the system detected 65% of the reference objects.

Initially, (Yang et al., 2016) employed the method proposed by (Hernández and Marcotegui, 2009) to split the point cloud into terrain and non-terrain portions. Then they detect the road surface and lane paintings, combining geometric and spectral features. The elements above the terrain were segmented into individual segments through an iterative scheme, which includes point classification, multi-rule segmentation, and merging adjacent segments. Finally, the semantic annotation framework, which benefits from features of various types (Point-based features, segment-based features, Point-based features in context-based objects and features), was applied to classify each segment into the desired object class.

As the segmentation and classification of objects is an open challenge when dealing with point clouds, the ultimate objective of this research is to advance the current state-of-the-art in detecting and classifying pole objects and road signs within urban environments. By automating this process, construction projects can benefit from increased efficiency, reduced time, and improved safety. The developed methodology aims to overcome the complexities associated with LiDAR point cloud classification, particularly the challenges posed by the similarity between different objects. Through the integration of advanced algorithms and machine learning techniques, the system will be capable of accurately identifying and categorizing pole objects and road signs, contributing to more effective urban planning and infrastructure development.

In summary, this study focuses on leveraging Mobile Terrestrial LiDAR and a neural network-based approach to semi-automatically detect and classify pole objects and road signs. The research takes place in an urban environment, using a comprehensive LiDAR dataset obtained from the campus of the Federal University of Paraná. By improving the accuracy and efficiency of detection and classification processes, this research aims to enhance urban infrastructure projects and contribute to effective urban planning.

II. Material And Methods

The detection of 3D objects in point clouds presents its own challenges, particularly in segmenting objects in urban areas, such as parts of buildings, people, poles, or trees. While detecting vertical elements is a relatively straightforward task, identifying poles becomes more complex, especially when dealing with small-diameter circular poles in comparison to larger objects like trees. Processing the large number of available points is a significant challenge, requiring substantial computational efforts. To overcome these challenges, the number of points to be processed was reduced at several steps of the process.

The proposed method for extraction and classification of poles and road signs can be divided in four steps: Data acquisition; Pre-processing; Detection of vertical elements; and modelling, which in turn is divided into modelling the pole and modelling the objects attached to the poles with neural networks.

Data acquisition and pre-processing

The data acquisition depends on the available mobile system. In our experiments, the average point density was 2,400 points per square meter, which proved sufficient for detailed analysis of the targeted poles and road signs. More details about data collection are provided in the “experiments” section.

Point cloud splitting aimed at better organization and management of the data, making it easier to process and analyze individual sections of the point cloud dataset. After the initial processing steps, each file in the dataset contained millions of points. Additionally, a metadata file accompanied each point cloud file, providing crucial information such as the start and end of the recording, the extent of the data, GPS time, point density, and measurements of the laser's offset relative to the IMU. To facilitate further analysis and improve computational efficiency, the set of measured point clouds needs to be reorganized and split into smaller slices along the trajectory of the vehicle. By dividing the dataset into slices along the vehicle's trajectory, it became possible to focus on specific segments of interest, enabling more efficient and targeted analysis of the data.

Considering the subset of points that belong to each separated slice, it was possible to classify the points into two classes: terrain and objects above the terrain. The classification of the terrain was accomplished using the Classify Hard Surface tool, which iteratively creates a triangular net model by adding the points

associated with the terrain. This approach is specifically designed for classifying areas captured with Mobile Terrestrial Laser Systems (MTLS) and helps streamline subsequent analyses. After eliminating the points of the terrain, a reduced point cloud is obtained.

Detection of vertical elements

The next step involved analyzing the point density of the reduced point cloud. This analysis focused on the 2D coordinates of the points, projecting them onto a regular horizontal 2D. This allows applying image processing techniques to detect clusters produced by vertical elements. For this purpose, cells with higher point density were identified, as points al vertical elements share their *xy*-coordinates. The efficiency of the detection process depends on the cell size of the grid, which influenced the resolution and accuracy of the analysis.

To estimate the cell size, it was considered the dimensions of the bounding box ($\Delta x, \Delta y$) of the point cloud and the point cloud density, according to Equations 1-3. The size of the bounding box is computed considering the minimal and maximal x and y coordinates (*Wmin*, *Wmax*, *Nmin*, *Nmax*).

$$\Delta x = \frac{(Wmax - Wmin)}{R} \quad (1)$$

$$\Delta y = \frac{(Nmax - Nmin)}{R}) \quad (2)$$

The grid resolution (R), Equation 3, is derived from the number of points and the 2D horizontal point cloud density.

$$R = \sqrt{\frac{Points\ by\ tile}{density\ m^2}} \quad (3)$$

After creating the empty grid, the reduced point cloud was projected into this grid, counting the number of points that fall into each cell. As a result, the total number of points corresponding to each cell was accumulated, as illustrated in Figure 1. Points associated with a pole, due to their closely matching planimetric coordinates, occupy the same cell within the grid. Consequently, this cell exhibits a high accumulation value, indicating the presence of a vertical element. This approach allows the identification of poles by detecting cells with significantly higher point accumulations, providing a visual representation of their spatial distribution within the dataset.

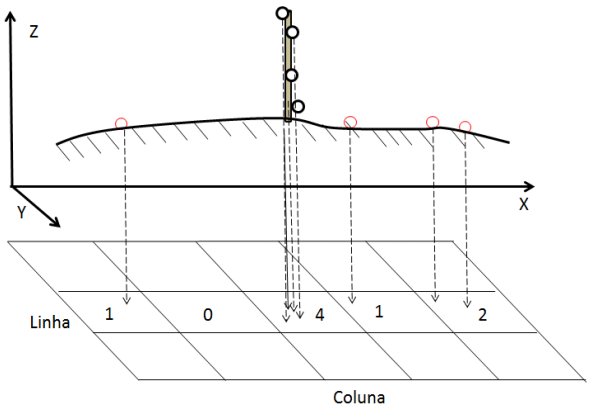

Figure 1 Representation the points of a vertical structure in a matrix.

The cumulation grid was thresholded to separate regions of high points concentration, with each region represented by a binary array containing 0's and 1's. The cells that that contained more points than the established threshold was labelled as 1, and the remaining as 0, which resulted in a binary image. The resulting grid allowed for a more organized representation of the data, enabling the identification and analysis of cells that contained vertical elements of interest. Then, the mathematical morphological closing operator was employed to fill in the holes within the regions containing poles and road signs. The closing operation involves a dilation followed by an erosion process. To perform this operation, a circular structuring element with a size of 20 pixels (equivalent to a radius of 20 pixels) was used.

After mathematical morphology, spatially continuous regions were labelled using the connected component algorithm. Connected component labeling also computes the number of objects in the image. Additionally, the centroid of each connected component was computed, which allowed computing the planimetric coordinates of the object.

Modelling

In the next step, the subset of points of each vertical object, segmented in the previous step, are classified as either pole or non-pole based on specific characteristics of the point cloud, such as height, orientation, density, and radius. It can be assumed, as displayed in Figure 2, that these objects can include two distinct components: the support and the top. Therefore, the initial step involved separating the support from the top to enable accurate calculation of the dimensions for each of these elements.

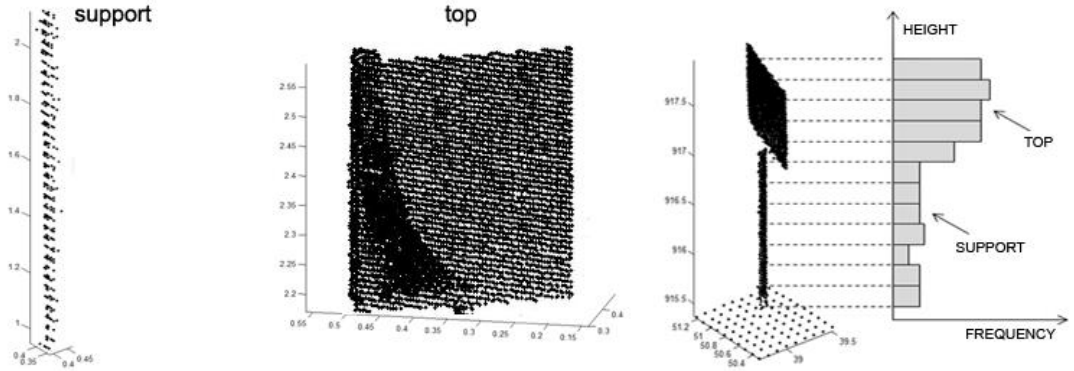

Figure 21 – A road sign segmented in support and top regions and the histogram.

In the initial stage, the height of each element is determined by extracting the maximum and minimum values of the Z coordinate. Additionally, a height histogram is computed to analyze the distribution of the points along the object. This process involves dividing the point cloud into vertical sections and counting the number of points within each section, as illustrated in Figure 2. Typically, the support pole exhibits a lower point density, whereas the attached object produces a higher point density. To construct the histogram, it is necessary to define the number of ticks, which depends on the height of each vertical section. The user can specify the height increment for each tick and the number of ticks can be calculated based on the desired height increment, using Equation 4,

$$ticks = ceil\left(\frac{Zmax - Zmin}{step}\right) + 1 \qquad (4)$$

To avoid disturbances occurring near the ground, such as stones or vegetation near the object, a minimum height was fixed from which the object would be analyzed. With it was defined the base, or the minimum height from which the object would be analyzed.

By analyzing the vertical frequency histogram, meaningful information about the object's structure and composition can be extracted. This histogram-based analysis aids in distinguishing between the support and top components, facilitating subsequent measurements and classification tasks.

Pole molde

After dividing the set into pole and attached object, it was possible to model the shape of the pole. The RANSAC (Random Sample Consensus) algorithm was applied to estimate the radius of the pole (Fischler, et al., 1981). This algorithm is known for its robustness in estimating model parameters, even in the presence of outliers within the point cloud data. It follows a series of iterative steps, as outlined below:

1. A height range around the mean height of the pole is selected to perform the analysis.
2. Among the points within the range, three points are chosen, and based on their coordinates, the center and radius of a horizontal circle passing through these points are computed.
3. It is verified if this circle accurately represents the contour of the pole. For this purpose, the distance between all other points within the range and the circle is calculated. If the estimation is correct, the difference would be zero. However, due to small variations in the point cloud, the difference is unlikely to be exactly zero. Therefore, the radius associated with the minimum difference is sought, indicating the best fit.
4. If the difference is non-zero, steps 2 and 3 are repeated, continuously storing the lowest error value and the corresponding radius achieved during the iterations.

By iteratively repeating this process and evaluating multiple candidate circles, the RANSAC algorithm can robustly estimate the radius of the support component. To ensure computational efficiency, a maximum limit of iterations needs to be set for the RANSAC algorithm. This limitation prevents long processing times while still allowing for accurate estimations. By employing the RANSAC algorithm, a reliable estimation of the radius of the support component can be obtained, even in the presence of noise or outliers in the point cloud data. This contributes to the accurate characterization and classification of poles in the subsequent stages of the

analysis. The algorithm's ability to handle outliers and noise in the point cloud data allows it to identify the most accurate representation of the pole's contour, as demonstrated by the red line in Figure 3.

In Figure 3, an example of this process is depicted. On one side of the pole, there are 13 points shown. The blue lines represent the various solutions generated by the RANSAC algorithm, each corresponding to a different set of three points. These solutions are candidate circles that pass through the selected points. The goal is to find the best fit circle that accurately represents the contour of the pole. The red line represents the best solution found by the RANSAC algorithm, which corresponds to the circle with the smallest difference between the distances of the points to the center.

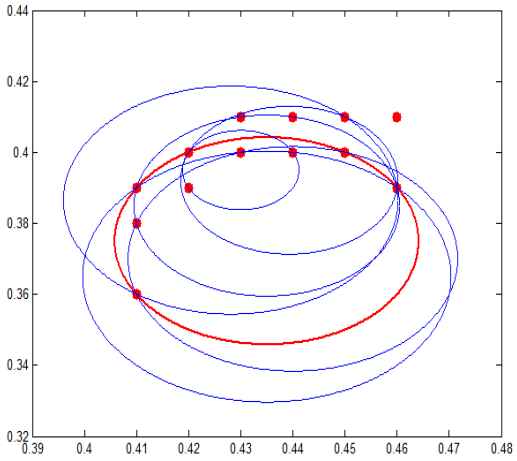

Figure 3 –Iterative process of RANSAC example.

Modelling the attached object

To analyze the attached objects (shields or lamps), the eigenvalues of the covariance matrix of the xyz coordinates of the point cloud was computed. The covariance matrix provides insights into the relationships and dependencies between the variables. The eigenvalues allow describing the three-dimensional variation of the cloud. If the points are evenly distributed in three-dimensional space, no predominant direction exists, and the eigenvalues could be equal. Conversely, if the size of the eigenvalues differs in magnitude, it indicates that there is one or two predominant directions in the point cloud, and therefore they can be used as shape descriptors. By analyzing the relative sizes of the eigenvalues, it is possible to determine the dominant directions that contribute the most to the variability of the top elements. This information helps in understanding the shape and structure of the objects under investigation and can assist in subsequent classification and analysis tasks.

In Figure 4, a comparison is shown between two types of elements: the cloud of points representing a lamp and a shield. The corresponding images of these elements are also depicted. The matrices displayed in the figure contain the eigenvalues λ1, λ2, and λ3. In this case, the third eigenvalue are smaller than the other ones, showing a planar tendency of the cloud. For the shield, the third eigenvalue is smaller because the shield is a flat surface. This information can be useful to classify the objects.

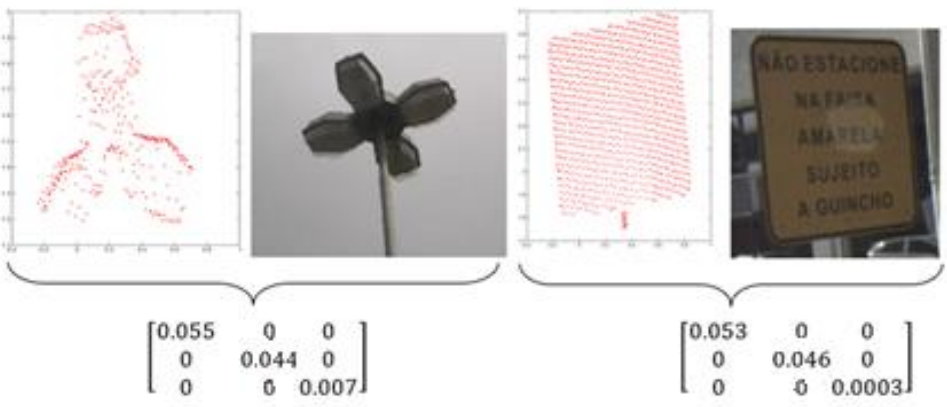

Figure 4 Example of eigenvalues of a pole and a road sign.

The spatial features and the eigenvalues were used as input of a neural network to classify the attached objects. This involves configuring various aspects such as the number of hidden layers, activation functions, number of training iterations, learning error threshold, training rates, and output format.

Data preparation plays a crucial role in the neural network workflow. It involves organizing the input data for the network, which includes parameters such as height, radius, and principal components of each pole and road sign. The training of the network is considered complete when the error falls below a predefined threshold or when a maximum number of iterations is reached (Pereira and Centeno, 2017). Overtraining, or overfitting, should be avoided as it can lead to a network that performs well on the training data but fails to generalize effectively to test data.

III. Experiments

The study area is located at the campus of the Federal University of Paraná in Curitiba, PR, displayed in Figure 5. The coordinates defining the area span from 25°27'15.49"S, 49°14'15.04"W to 25°26'45.31"S, 49°13'47.49"W. The scanning process encompassed 2.3 linear kilometers and lasted two hours. The location map provided in Figure 5 represents a composite image combining intensity and hypsometry information. This map offers a visual representation of the terrain characteristics and elevations within the study area. By integrating intensity and hypsometry data, a comprehensive understanding of the topography and features of the block access road can be obtained.

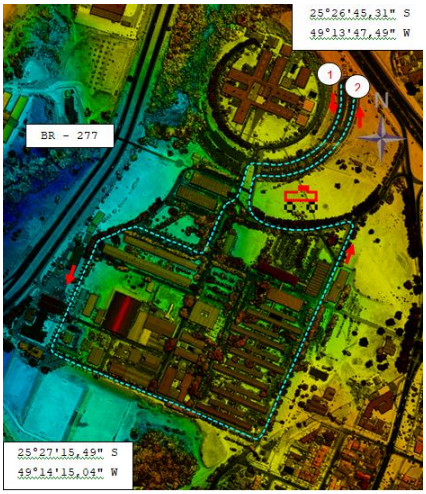

Figure 5 - Study Area (Intensity and Hypsometric Map)

The data utilized in this study were collected using the Pegasus One Mobile System, a Swiss system developed by Leica Geosystems and introduced at the Hexagon Live 2013 event in the United States. It became available in Brazil in 2014. The Pegasus One Mobile System comprises a LiDAR sensor, a GNSS receiver, an IMU, a DMI, and a unique advantage over other systems: six digital metric cameras strategically positioned on the vehicle platform, including front, rear, and side-facing cameras. The data was acquired using the mobile system in a single direction, starting from point 1 and ending at point 2, as depicted in Figure 5. The data acquisition was conducted at the allowed speed of 30 km/h to maintain accuracy. The average point density was 2,400 points per square meter, which proved sufficient for detailed analysis of the targeted poles and road signs.

Figure 6 - Pegasus One System components (Hexagon, 2014)

In the pre-processing stage the point cloud was computed using the software provided by Leica. The processing was performed using an Intel Core i7 computer with a 3.2GHz processor, 32GB of RAM. The IMU/GNSS trajectory was processed using Novatel's Inertial Explorer software, which is crucial for achieving accurate results in Mobile Terrestrial Laser System applications. Since surveys are often conducted in areas with GPS signal obstructions, such as trees and buildings, processing the trajectory becomes complex due to potential gaps in information. Following GPS/IMU processing, the point cloud generation was performed using Automatic Post Processing® software. This software utilized the smoothed trajectory generated by Inertial Explorer® for georeferencing the point cloud and aligning the six metric cameras of the system. All these steps were carried out to ensure a reliable IMU/GNSS solution and high-quality raw data for subsequent analysis. Therefore, all procedures were taken for a good IMU / GNSS solution and good raw data.

Following the proposed methodology, the point cloud was split into several slices along the trajectory to reduce the data volume. As illustrated in Figure 8a. Each slice contained approximately 10 million points, as depicted in Figure 8b.

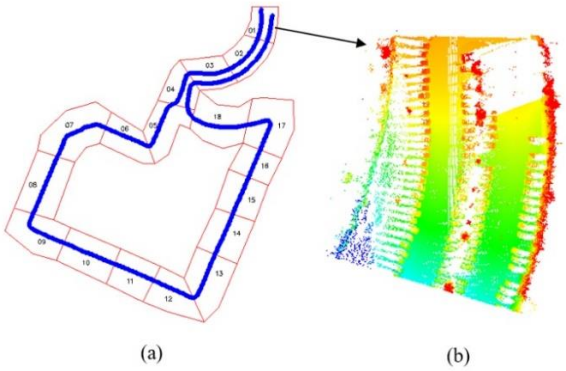

Figure 8 (a) Map Tiles and Trajectory (b) Point Cloud Tile

After eliminating the points that belong to the ground and segmenting the point cloud into small sets that belong to single objects, the number of points to be analyzed was reduced significantly. Projecting the points into the vertical grid and detecting clusters that are related to vertical objects allows separating the points that belong to the same object and the location of each object. An example of the resulting locations, represented by crosses, is illustrated in Figure 9. This example demonstrates the successful detection of nine elements (i.e., poles). The points belonging to the same connected component were stored in a different file, which enabled the analysis of the isolated object in the next steps.

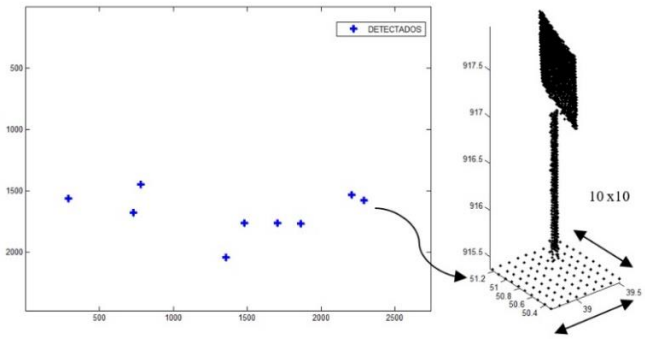

Figure 9- Result of label regions result.

The next step is to analyze the vertical histogram of the point cloud of the segment. An example of a histogram is shown in Figure 10. The height of this object is 2.63 meters. Applying equation 2. It is possible to compute the number of ticks, 54 ticks, i.e., each step has 0.05 meters. To avoid the influence of lower vegetation, the analysis was restricted to points above 1m.

It is assumed that the top of the top is characterized by a significant jump in the histogram values, since the top has a larger area. As shown in Figure 10, the average density calculated along the carrier is 0.05. The beginning of the top is defined by the first location which has a higher density of points, which in the example presented is 0.15 points per m2.

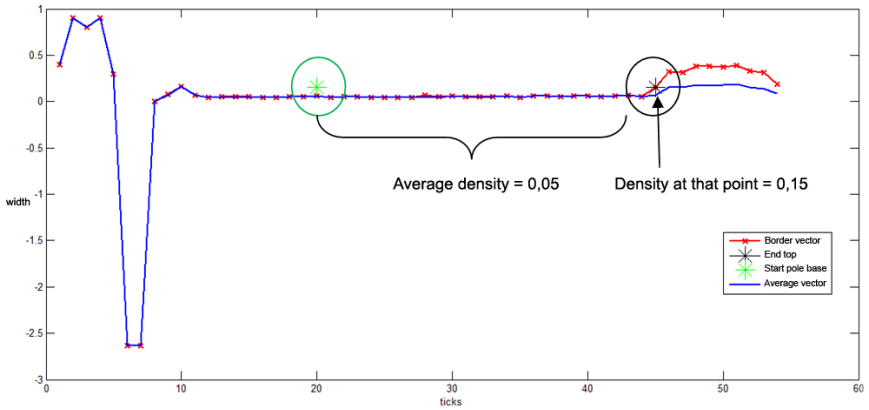

Figure10 –Average density calculation example.

The histogram enabled to separate the pole from the attached object. The pole was modeled as a cylinder and the attached object was classified with neural networks, using the spatial features as input. Seven different classes of attached objects were previously identified in the study region. These classes were sequentially numbered from 1 to 7, as illustrated in Figure 11. Specifically, lamps are represented by numbers 1 to 4, while shields by numbers 5 to 7.

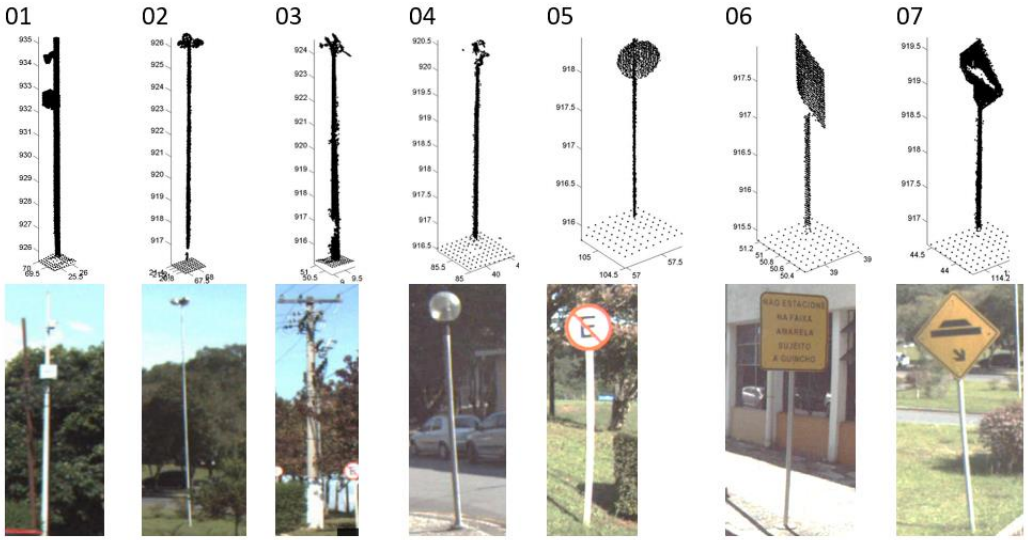

Figure - 2 Type of elements of poles and road signs

For this study, a feedforward architecture is employed, which utilizes the backpropagation training algorithm. This algorithm systematically adjusts the weights in the network to optimize classification performance. The network architecture consists of one hidden layer with 10 neurons and an output layer with a single neuron. The activation function used in this study is the tangent sigmoid (tansig). To ensure sufficient training data, it is recommended to have several training examples at least double the number of input neurons. In this study, 32 elements were selected as training data, exceeding the minimum requirement. This larger dataset accounts for the partitioning strategy employed by Matlab®, which allocates 20% for testing, 20% for validation, and 60% for training.

IV. Results

The detection of elements was carried out using the 2D density analysis methodology. A threshold was determined based on the number of points within each section. Any vertical element that exceeded this threshold was considered a potential candidate. Figure 12 illustrates the geolocation of the detected poles and road signs as identified by the routine. Through this methodology, the routine successfully identifies and localizes the poles and road signs within the scanned area. The geolocation information, combined with the profile view images, provides valuable insights into the spatial distribution of these elements.

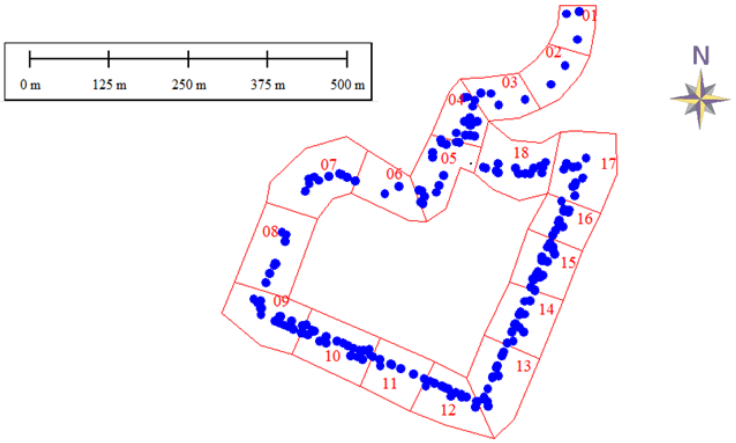

Figure - 3 Pole and road signs detected

The confusion matrix in Table 01 presents the results of the first detection, showing the number of elements classified as lamps and shields. The precision of 84.76% indicates that most of the detected elements were correctly classified. However, the recall value of 64.02% suggests that some elements were not accurately detected, leading to false negatives.

Table 01 *Confusion* matrix - Quantity of elements

Class		Predicted		Precision	Recall
		True	False		
Actual	Positive	178	32	84,76%	64,02%
	Negative	100			

The precision metric reflects the proportion of correctly classified elements among the total elements detected. In this case, it indicates that 84.76% of the detected elements were indeed lamps or shields. On the other hand, the recall metric represents the proportion of correctly detected elements compared to the total number of actual elements. With a recall value of 64.02%, it indicates that some elements were missed or incorrectly identified during the detection process.

The detection performance can be further improved by fine-tuning the algorithms, adjusting the threshold values, or considering additional features for classification. By addressing the limitations highlighted by the recall metric, the overall accuracy of the detection system can be enhanced.

To identify the error sources, the misclassifications were visually analyzed. The following problems were detected (Figure 13):

a) Road sign with a person next to it: In this case, the presence of a person near the road sign can lead to confusion during detection.

b) Pole under the tree: The presence of vegetation, such as a tree, can partially obstruct the view of the pole, making it more challenging to accurately detect.

c) Incomplete pole: Sometimes, poles may be partially occluded or damaged, resulting in incomplete structures. These incomplete elements pose a challenge for accurate detection.

d) Incomplete shield: Like incomplete poles, road signs that are damaged or missing certain components may not be accurately detected without proper filtering.

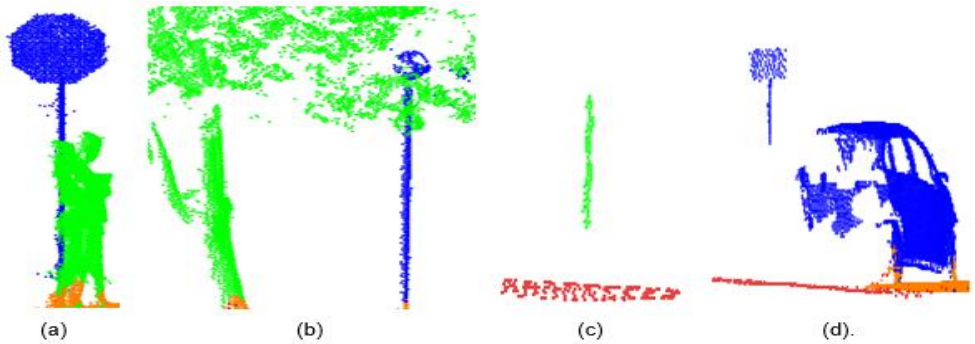

Figure - 4 Examples of detection problems

Before applying the neural networks for classification, point clouds of incomplete or occluded objects were manually discarded. So, the classification was applied only to complete sets. The aim is to address specific challenges and improve the accuracy of the classification performed by the neural networks. It helps to reduce false positives and improve the overall detection and classification results of the elements of interest. By removing incomplete elements, the dataset was refined to ensure a more focused and reliable analysis. This approach provides a clearer assessment of the neural networks' efficiency in classifying the elements. The subsequent analysis and evaluation of the neural networks' performance will be based on this refined dataset, which aims to provide more accurate and reliable results in classifying the poles and road signs.

The classification process involved dividing the elements into eight classes, with classes 1 to 7 representing the poles with lamps and poles with shields. Vertical elements without attached object were previously separated into a different class (8). To assess the effectiveness of the neural networks, elements without a top component and incomplete elements were excluded from the analysis. The training set represented 26% of the total 152 elements selected for the study. The training was conducted using the hyperbolic tangent function, as previously employed. The dataset chosen for RNA Backpropagation was used for training the neural network. After 17 iterations, the neural network reached convergence.

Table 02 displays the confusion matrix, which indicates the number of correct and false classifications. The overall classification accuracy is 98.02%, demonstrating the effectiveness of the neural network in accurately classifying the elements. However, there were a few misclassifications. In class 4, one element was classified as class 5, likely due to the similarity in their respective heights. Something similar was observed in class 7, where elements were sometimes confused with class 6. This confusion can be attributed to the resemblance between the characteristics of these classes. Despite these occasional misclassifications, the overall accuracy of 98.02% confirms the success of the neural network in classifying most elements within the refined dataset.

Table 02 - Confusion matrix – Percentage of elements by class (152 elements);

Class	1	2	3	4	5	6	7	Total
1	2	0	0	0	0	0	0	2
2	0	1	0	0	0	0	0	1
3	0	0	9	0	0	0	1	10
4	0	0	0	56	1	0	0	57
5	0	0	0	0	68	0	0	68
6	0	0	0	0	0	8	0	8
7	0	0	0	0	0	1	5	6
TOTAL	2	1	9	56	69	9	6	152

Table 03 presents the evaluation of the pole objects classification. The table includes various performance metrics for each class. In terms of true positives (VP), all classes achieved satisfactory results, indicating that the neural network successfully identified the respective elements. False negatives (FN) were observed only in class 3, where one element was mistakenly classified as another class. False positives (FP) were minimal, with class 6 having one incorrect classification.

Table 03 - Evaluation of the pole objects classification.

Class	VP	FN	FP	Total	Precision	Recall
1	2	0	0	2	100.00%	100.00%
2	1	0	0	1	100.00%	100.00%
3	9	1	0	10	90.00%	100.00%
4	57	0	0	57	100.00%	100.00%
5	68	0	0	68	100.00%	100.00%
6	8	0	1	8	100.00%	88.89%
7	5	1	1	6	83.33%	83.33%

The precision metric measures the accuracy of positive predictions, representing the percentage of correctly classified elements among all elements predicted as positive. All classes achieved high precision scores, ranging from 83.33% to 100.00%. Class 7 had the lowest precision of 83.33%, indicating that some elements in this class shared similar characteristics with other classes, leading to misclassifications.

The recall metric assesses the ability of the classifier to identify all relevant elements, representing the percentage of correctly classified elements among all actual positive elements. All classes achieved perfect recall scores of 100.00%, except for class 6 with a recall of 88.89%. This suggests that one element in class 6 was not identified by the classifier, possibly due to its similarity with other elements.

The classification results demonstrate a high level of accuracy and successful identification of the majority of pole objects. However, class 7 exhibited slightly lower precision and recall scores due to the similarity of its elements with other classes.

V. Conclusion

This study demonstrated the feasibility of using a point cloud, collected with a mobile terrestrial laser system, to automatically detect and classify poles with lamps and shields located near streets as part of urban furniture. Despite the urban setting and the visual detectability of the objects, the mathematical analysis posed challenges due to obstacles such as trees, cars, and pedestrians. It was necessary to refine parameters and, in some cases, exclude complex scenarios to improve the detection accuracy.

It was observed that the variables of height, radius, and the eigenvalues computed from the variance-covariance matrix were sufficient for the classification of objects using an artificial neural network. The classification process achieved an overall accuracy of 90%, indicating the effectiveness of the proposed procedures.

However, it is important to note that the results are strongly affected by the presence of parked cars and pedestrians along the scene. Therefore, it is recommended to conduct the profiling at a time and day when there are fewer obstructions to ensure more accurate results.

Furthermore, this study opens possibilities for extending the methodology to detect and classify other objects beyond the scope of this research. Future works can explore the application of similar techniques to detect and classify different types of objects using point cloud data.

Overall, the findings of this study contribute to the advancement of automated object detection and classification using mobile terrestrial laser systems, providing insights for further research and potential applications in various domains.

Acknowledgements

This research was supported by CNPQ – Conselho Nacional de Desenvolvimento Científico e Tecnológico. We thank Esteio Engineering and Aerial Surveys and Leica Geosystems for sharing their data for this research.

References

[1]. Chen, Q. Airborne Lidar Data Processing And Information Extraction. Photogrammetric Engineering And Remote Sensing, V. 73, N. 2, P. 109-117, 2007.

[2]. Dias, M. J. Et Al. Are Brazilian Cities Ready To Develop An Efficient Urban Freight Mobility Plan? Brazilian Journal Of Urban Management, V. 10, N. 3, P. 587-599, 2018.

[3]. Fernandes, D. Et Al. Point-Cloud Based 3D Object Detection And Classification Methods For Self-Driving Applications: A Survey And Taxonomy. Information Fusion, V. 68, P. 161-191, 2021.

[4]. Fischler, M. A.; Bolles, R. C. Random Sample Consensus: A Paradigm For Model Fitting With Applications To Image Analysis And Automated Cartography. Communications Of ACM, V. 24, N. 6, Jun. 1981.

[5]. Hexagon. Leica Geosystems. Capture Platforms: Leica Pegasus Two. Disponível Em: Https://Leica-Geosystems.Com/Pt-Br/Products/Mobile-Sensor-Platforms/Capture-Platforms/Leica-Pegasus_Two, 2014.

[6]. Hernández, J.; Marcotegui, B. Filtering Of Artifacts And Pavement Segmentation From Mobile Lidar Data. In: ISPRS Workshop Laserscanning 2009, 2009.

[7]. Manandhar, D.; Shibasaki, R. Vehicle-Borne Laser Mapping System (VLMS) For 3-D GIS. In: IGARSS 2001. Scanning The Present And Resolving The Future. Proceedings. IEEE 2001 International Geoscience And Remote Sensing Symposium (Cat. No. 01CH37217), V. 5. IEEE, 2001.

[8]. Pereira, G. H. De A.; Centeno, J. A. Assessment Of Training Sample Size For Artificial Neural Networks In Supervised Image Classification Using Spectral And Laser Scanner Data. Boletim De Ciências Geodésicas, V. 23, N. 2, P. 117-131, Curitiba, 2017.

[9]. Yang, B. Et Al. Two-Step Adaptive Extraction Method For Ground Points And Breaklines From Lidar Point Clouds. ISPRS Journal Of Photogrammetry And Remote Sensing, V. 119, P. 373-389, 2016.